1 January 2000

Optics Communications 173 (2000) 185–193

OPTICS COMMUNICATIONS

www.elsevier.com/locate/optcom

Optical implementation of the sliced orthogonal nonlinear generalized correlation for images degraded by nonoverlapping background noise

Pascuala Garcia-Martinez [1], Henri H. Arsenault *, Sébastien Roy

COPL, Universite Laval, Ste-Foy, Qc, Canada G1K 7P4

Received 10 August 1999; accepted 26 October 1999

Abstract

We study the performance of the sliced orthogonal nonlinear generalized (SONG) correlation for images degraded by clutter and nonoverlapping background noise. We present experiments on the optical implementation of the SONG correlation obtained by means of a joint transform correlator. Nonoverlapping noise does not contribute to the SONG correlation, and the SONG auto-correlation peak is insensitive to changes of background patterns around the target and experiments show that this is not the case for other methods. © 2000 Elsevier Science B.V. All rights reserved.

Keywords: Pattern recognition; Nonlinear correlations; Joint transform correlator; Optical processing

1. Introduction

In many optical pattern recognition applications the input scene has disjoint noise, that is, the input noise does not overlap the target. Some optimal filters or processors have been devised to deal with such pattern recognition cases. Javidi and Wang [1] showed that classical measures of correlation performance are inadequate for images with nonoverlapping noise. They also showed that the recognition performance could be greatly improved with filters designed specifically for nonoverlapping noise [2]. Those filters are designed to optimize the output signal according to certain metric criteria such as the minimization of the probability of detection error [3] or the minimization of the mean squared difference between the correlation output and a desired output delta function [4]. Those methods have been developed to deal with images degraded by nonoverlapping background noise, but most such methods require segmentation of the targets or are nonlinear and therefore lose the shift invariant property.

We recently proposed a nonlinear correlation method based on gray level detection. The sliced orthogonal nonlinear generalized (SONG) correlation is equivalent to counting the number of pixels that have the same gray levels in two images and are at the same positions as the target to be detected [5]. The SONG correlation is based on a general SONG

* Corresponding author. Tel.: +1-418-656-2650; fax: +1-418-656-2623; e-mail: arseno@phy.ulaval.ca

[1] On leave from Dpt. D'Òptica, Universitat de València, c/Dr. Moliner 50, E-46100 Burjassot, Valencia, Spain.

PII: S0030-4018(99)00649-5

decomposition, which is an elementary orthogonal representation of an image. We showed that classical matched filters, binary filters, and other nonlinear correlation like optical morphological correlation [6] can be expressed in terms of the SONG decomposition.

If a target is corrupted by nonoverlapping background noise or by disjoint clutter, such noise sources will not have any influence on the auto-correlation because of the orthogonality property of the SONG auto-correlation, so the SONG correlation is unaffected by any background that does not overlap the target.

One focus of this paper is the first optical implementation of the SONG correlation. Because the SONG correlation can be expressed as a sum of linear correlation, we can easily implement the SONG correlation with a joint transform correlator.

2. The SONG decomposition and the SONG correlation

We now briefly review the definitions of the SONG decomposition and correlation. Any two-dimensional image $f(x,y)$ with discrete gray levels can be decomposed into a sum of orthogonal elementary images $\{e_m(f)\}$ satisfying the orthogonality property

$$e_m(f)\,e_n(f) = 1 \text{ if } m = n$$
$$e_m(f)\,e_n(f) = 0 \text{ if } m \cdot n. \tag{1}$$

Each sub-image $\{e_m(f)\}$ represents a gray level slice of the object. We define the sliced orthogonal nonlinear generalized (SONG) decomposition of $f(x,y)$ as

$$f(x,y) = \sum_{q=1}^{Q-1} q e_q(f) \tag{2}$$

where Q is total number of gray levels in the image and the basis is defined as

$$e_q(f) = \begin{cases} 1 & f(x,y) = q \\ 0 & \text{otherwise} \end{cases}. \tag{3}$$

Note that each object point is characterized by only one gray level, so that each q-slice is orthogonal to all of the others. By considering a three-dimensional space with coordinates (x,y,q), the method can be interpreted as placing planes parallel to the (x,y) coordinate plane of the image; each plane then 'slices' the function in the area of intersection. All of these areas form disjoint sets of pixels, each set corresponding to one gray level.

The SONG correlation Ω_{gf} is based on the binary SONG decomposition between a function $g(x,y)$ and an object prototype $f(x,y)$, and is defined as

$$\Omega_{gf}(x,y) = \sum_{q=1}^{Q-1} W(q,\chi)\,e_q(g) \otimes \sum_{k=1}^{Q-1} W'(k,\chi)\,e_k(f) \tag{4}$$

where $W(q,\chi)$ and $W'(k,\chi)$ are weighed correlation factors and χ is a parameter that may depend on detection functions or other metrics and where $\otimes$ denotes the linear correlation operation. In the absence of any a priori information about the input scene, there is no reason to put any different weights on the binary slices. So the SONG correlation definition that we shall consider in this paper is

$$\Omega_{gf}(x,y) = \sum_{q=1}^{Q-1} \left[e_q(g) \otimes e_q(f) \right] \tag{5}$$

where $W(q,\chi) = W'(k,\chi) = 1$ and $q = k$, so we are considering only the corresponding gray level binary slices for the $g(x,y)$ and for the $f(x,y)$ functions.

The definition of the SONG auto-correlation (Ω_{ff}) means that the operation can be viewed as a function that counts the total number of non-zero pixels (or points) in an image. Indeed, the SONG correlation process consists of separately correlating each binary slice from the image with each binary slice of the prototype corresponding to the same gray level, and then summing the correlation values. Because the base $\{e_q(f)\}$ is orthogonal in the $f(x)$ domain, each correlation value is proportional to the number of pixels that are common to both slices. For the auto-correlation, the sum for all the gray levels yields the total number of pixels in the object. So the SONG auto-correlation is equivalent to a counting operation: the height of the auto-correlation peak (in the absence of noise) is equal to the number of pixels in the object, and in the case of false targets, the height of the correlation peak is equal to the number of pixels that have the same gray level values in the target and in the prototype. Note that there could be objects that have the same number of pixels but that look totally different from the reference object. But the counting operation that results from our cross-correlation measures the number of equal-valued pixels that are in the same locations for both objects, which is a good measure of similarity.

3. The SONG correlation for cluttered images and for nonoverlapping background noise

Consider an input signal $s(x,y)$ that can be expressed as

$$s(x,y) = f(x,y) + n(x,y) \tag{6}$$

where $f(x,y)$ is the target and $n(x,y)$ is background noise that is spatially disjoint from the target (does not overlap the target).

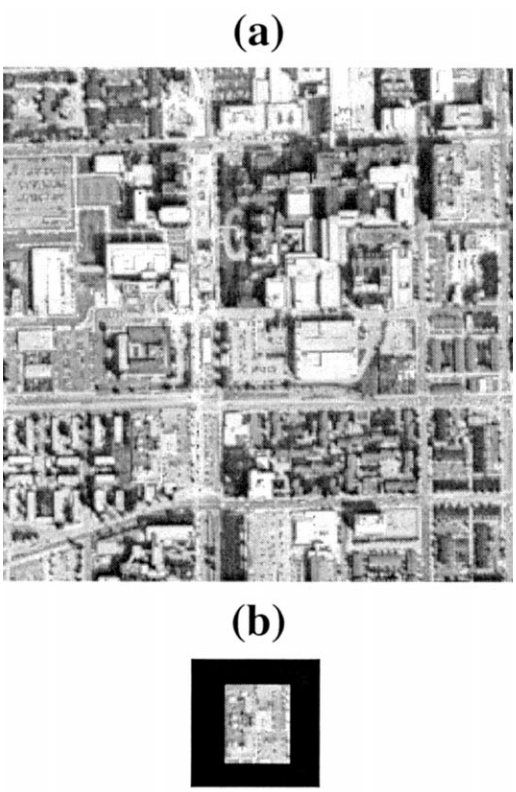

Fig. 1. (a) Input scene for the cluttered image detection, where two targets are in the scene; and (b) target to be detected in the scene (Fig. 1(a)).

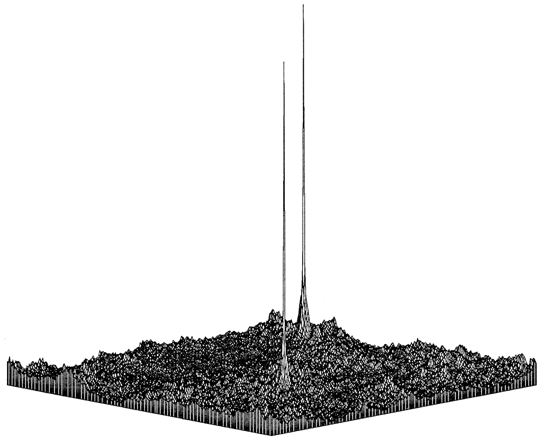

Fig. 2. 3-D plot for the SONG correlation of Fig. 1(a).

Because of the definition of the SONG correlation (see Eq. (5)), we can express the SONG correlation between $s(x,y)$ and $f(x,y)$ as

$$\Omega_{sf}(x,y) = \Omega_{ff}(x,y) + \Omega_{nf}(x,y). \tag{7}$$

Note that Eq. (7) is only valid if the noise background has no influence on the correlation peak. This is true for the SONG correlation because the SONG orthogonal auto-correlation will take into account the gray levels the target independently of the background. Eq. (7) is also true for the matched filter at the linear correlation but only at the origin.

For the SONG correlation, not only has the background no influence on the SONG correlation, but in addition the correlation between $n(x,y)$ and the target $f(x,y)$ is equal to zero. Then Eq. (7) can be written as

$$\Omega_{sf}(x,y) = \Omega_{ff}(x,y). \tag{8}$$

This is only true for a correlation which counts the number of pixels that have the same gray levels at the same positions, that is the SONG correlation. Eq. (8) is only true for the case of nonoverlapping background noise. Another important remark is that Eq. (8) is verified not only at the origin (0,0) but over the whole correlation plane (x,y). This is the main difference with the linear correlation, where Eq. (8) applies only at the origin.

We carried out some computer experiments to determine the stability of various correlation methods in the presence of disjoint noise. Fig. 1(a) is the

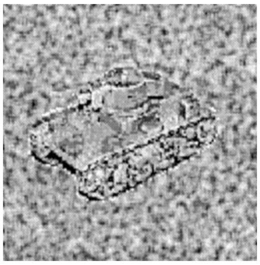

Fig. 3. Reference object degraded by correlated Gaussian disjoint noise.

input image containing two identical buildings shown in Fig. 1(b), surrounded by correlated noise. The SONG correlation is shown in Fig. 2 where the two targets are clearly detected, despite the fact that the two buildings are extremely difficult to spot by eye.

We now consider the stability of the SONG correlation for the detection of a target in the presence of disjoint patterns. Fig. 3 contains a target (a tank) that is corrupted by correlated Gaussian disjoint noise. The background is a Gaussian noise distribution with a mean of zero and various values of the deviation σ. This parameter is a measure of the energy of the pattern where a greater value of σ represents a brighter background.

Javidi and Wang [1] showed that the classical signal to noise ratio (SNR) is not a good measure of the system performance, because it goes to infinity for nonoverlapping background noise. So, in order to study the performance of the SONG correlation for this kind of noise, we study two parameters: the peak to correlation energy [7] (PCE) and what we define as the auto-correlation noise to signal ratio (ANSR).

The PCE measures the sharpness of the correlation peak and it is defined as

$$PCE = \frac{|c(0,0)|^2}{\int\int_{\Sigma} |c(x',y')|^2 \mathrm{d}x' \mathrm{d}y'} \tag{9}$$

where $c(x,y)$ can be the SONG correlation or the common linear correlation. A high value of PCE means a sharp correlation peak.

We define the ANSR as

$$ANSR = \frac{Autocorr_{(s,f)}(0,0)}{Autocorr_{(f,f)}(0,0)}. \tag{10}$$

The numerator of Eq. (10) represents the value of the auto-correlation at the origin when the image is corrupted. The denominator represents the value of

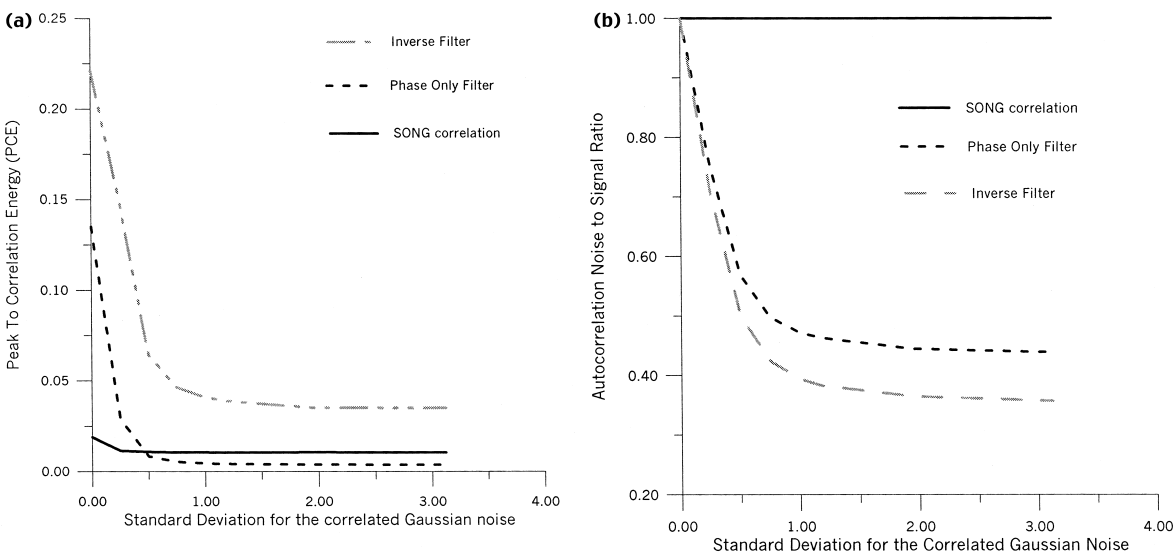

Fig. 4. (a) Performance of the *PCE* for the SONG correlation (solid curves), the phase only filter (short-dashed curves) and the inverse filter (long-dashed curves) when the standard deviation of the background input noise is varied; and (b) performance of the *ANSR* for the SONG correlation (solid curves), the phase only filter (short-dashed curves) and the inverse filter (long-dashed curves) when the standard deviation of the background input noise is varied.

the auto-correlation at the origin for a noise-free target. When the noise has a strong contribution, the numerator goes to zero, because the auto-correlation value will be reduced in the presence of noise sources. We show that the SONG auto-correlation peak at the origin does not change, and so the ANSR is invariant under energy changes of the noise. On the other hand, for the POF and for the inverse filter (IF), the ANSR is strongly affected. Javidi and Wang [2] also studied the variation of the correlation-peak intensity for the case of POFs and other nonlinear optimum filters.

Fig. 4 (a) shows the PCE for the SONG correlation, the POF and the IF, when the input image is corrupted by various levels of disjoint correlated Gaussian noise. The PCE for the SONG correlation is almost constant for the different background patterns. On the other hand, the POF and the IF are strongly affected when the noise level varies. Note that the IF has a better PCE than the SONG correlation. This result is to be expected because the IF is optimum under this parameter. But, it is not as stable as the SONG correlation.

Fig. 4(b) is a plot of the variation of the auto-correlation peak (ANSR) due to the noise. Whereas the auto-correlation peak value for SONG correlation is invariant under noise changes, both the POF and the IF are strongly affected by the noise, that is the auto-correlation energy for those filters decreases with increasing noise levels.

4. Optical implementation of the SONG correlation

In a previous section, we showed that the SONG correlation has excellent performance against disjoint noise, in fact is insensitive to such noise. In this section we show that the noise has no influence on the discrimination capability of the SONG correlation. Moreover, the SONG correlation can be easily implemented optically using a simple joint transform correlator (JTC).

From Eq. (5), the SONG correlation is defined as the sum of the amplitudes of the linear correlations between the corresponding binary slices of the input scene and of the target. This amplitude summation can be carried out by a JTC.

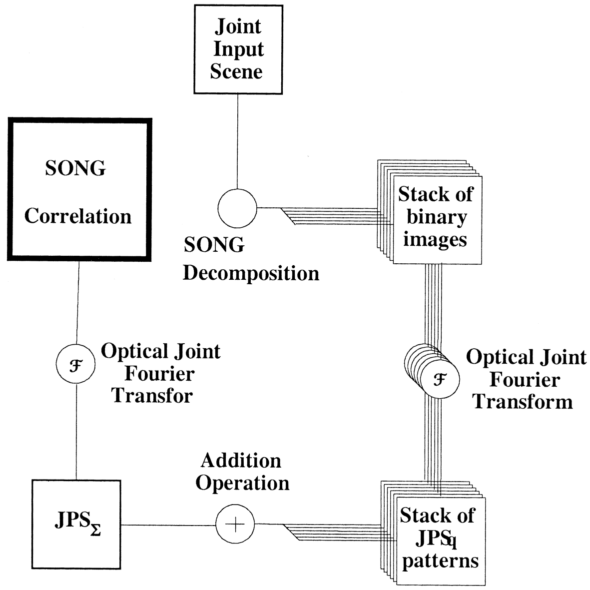

Fig. 5. Block diagram of the optoelectronic SONG correlation.

Let $f(x+x_0,y)$ and $g(x-x_0,y)$ be the reference and the input scene objects centered at $(-x_0,0)$ and $(x_0,0)$, respectively. The SONG correlation can be implemented optically using the same system as for the morphological correlation [6]. The setup is shown in Fig. 5. Each pair of elementary binary joint input slices (one slice from the reference object and one from the input scene) are placed next to each other in the input plane. For each pair, the joint power spectrum is performed. The summation of the joint power spectrum for all the slices is

$$\begin{aligned} JPS_\Sigma(u,v) = {} & \sum_{q=1}^{Q-1} JPS_q = \sum_{q=1}^{Q-1} |FT\{e_q(f)\}|^2 \\ & + \sum_{q=1}^{Q-1} |FT\{e_q(g)\}|^2 \\ & + \sum_{q=1}^{Q-1} FT\{e_q(f)\}^* FT\{e_q(g)\} \\ & \times \exp[-i2\phi_q(u,v)] \\ & + \sum_{q=1}^{Q-1} FT\{e_q(f)\} FT\{e_q(g)\}^* \\ & \times \exp[i2\phi_q(u,v)] \end{aligned} \tag{11}$$

where FT is the Fourier transform and $\phi(u,v) = (2\pi u x_0)/(\lambda f)$, with f being the focal length of lens and λ the wavelength of the illumination coherent light. The Fourier transform of the third term of Eq. (11) yields the SONG correlation. In addition the Fourier transform of the fourth term is the conjugate of the SONG correlation.

Note that although each optical linear correlation is carried out in parallel, the binary correlations are carried out sequentially. However this SONG correlation could be implemented in a single step using the method developed for the optical implementation of the morphological correlation [8].

5. Optical experimental results

The spatial light modulator (SLM) that we use for the optical experiments is a VGA LCTV from CRL Smetic Technology. We have considered three kinds

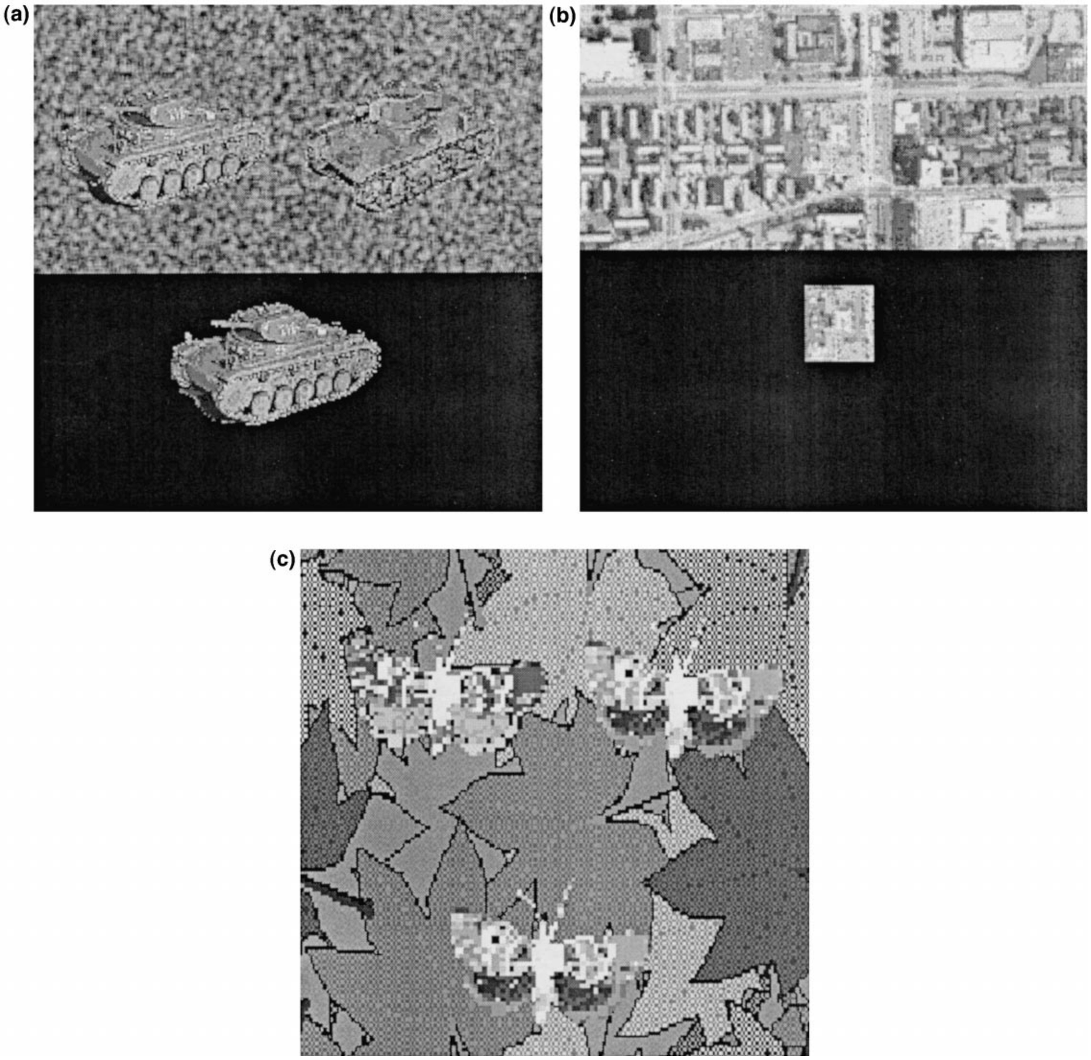

Fig. 6. (a) Joint input scene containing the input scene (top) and the reference object (bottom); (b) joint input scene containing the input scene (top) with the cluttered image and the reference object (bottom); and (c) joint input scene with the background covering the whole input plane. The input scene is placed on the top and the reference object is on the bottom of the figure.

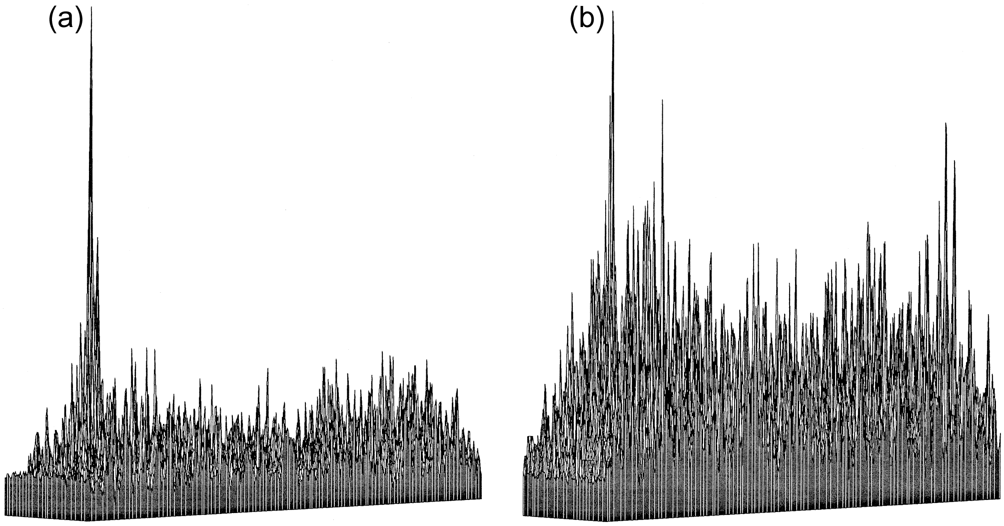

Fig. 7. (a) Experimental output plane containing the optical SONG correlation of the scene shown in Fig. 6(a), where the 3-D plots cover an area around the correlation peaks; and (b) experimental output plane containing the optical linear correlation of the scene shown in Fig. 6(a), where the 3-D plots cover an area around the correlation peaks.

of images for the optical implementation, shown in Fig. 6(a)–Fig. 6(c). The images have 8 gray levels. We study the discrimination capability of the SONG correlation when the object to be detected is found in

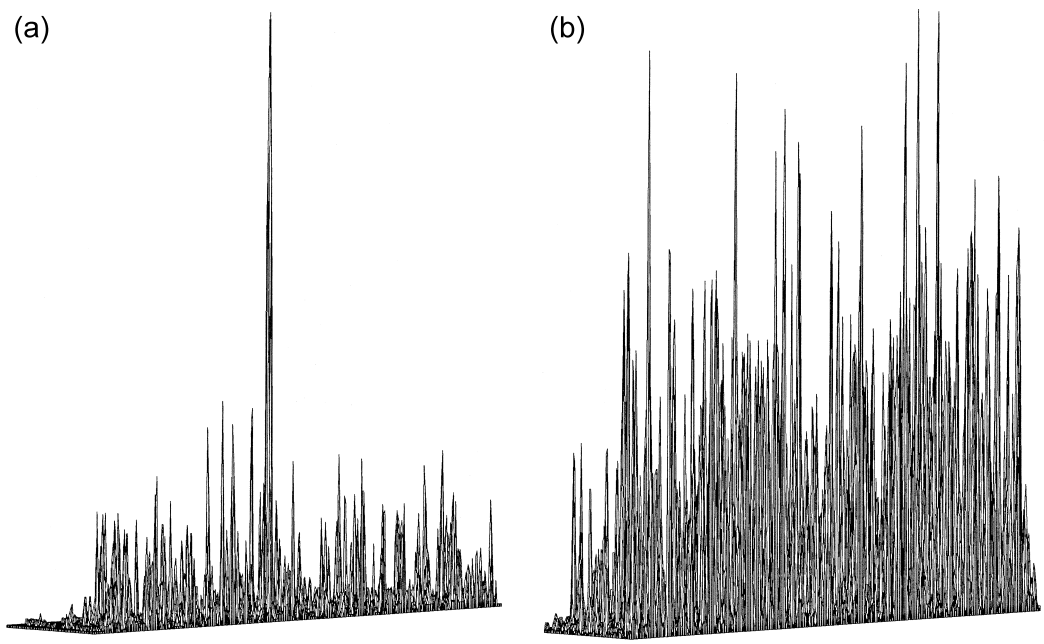

Fig. 8. (a) Experimental output plane containing the optical SONG correlation of the scene shown in Fig. 6(b), where the 3-D plots cover an area around the correlation peaks; and (b) experimental output plane containing the optical linear correlation of the scene shown in Fig. 6(b), where the 3-D plots cover an area around the correlation peaks.

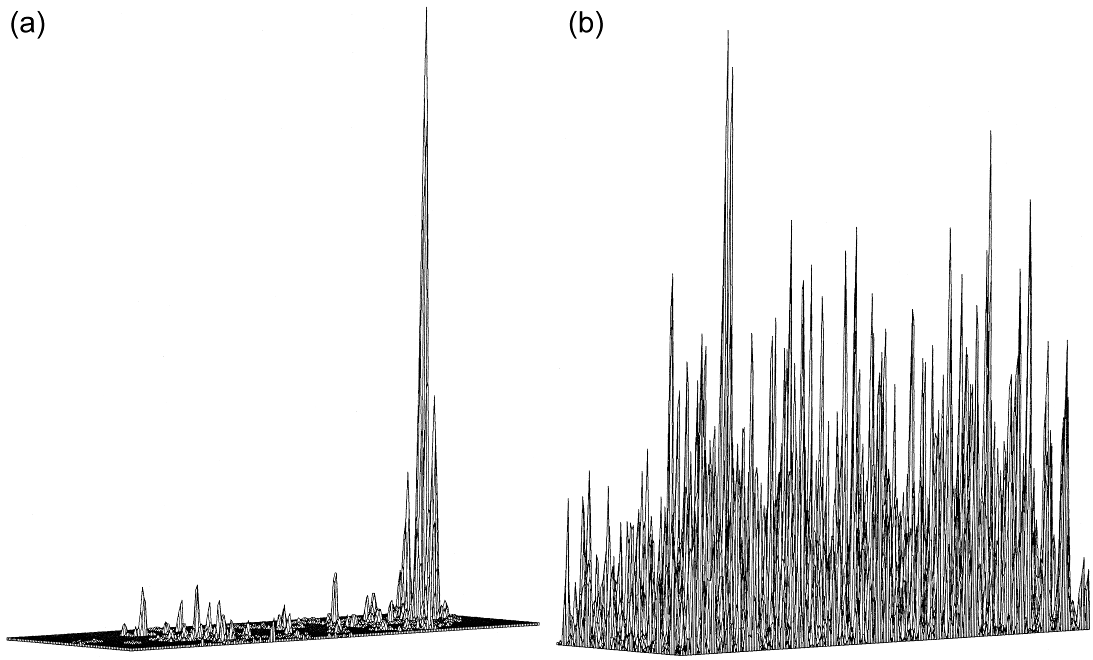

Fig. 9. (a) Experimental output plane containing the optical SONG correlation of the scene shown in Fig. 6(c), where the 3-D plots cover an area around the correlation peaks; and (b) experimental output plane containing the optical linear correlation of the scene shown in Fig. 6(c), where the 3-D plots cover an area around the correlation peaks.

the presence of other objects and of disjoint noise. Fig. 6(a) contains two tanks that are surrounded by correlated disjoint noise. Fig. 7(a) shows the result for the SONG correlation, and Fig. 7(b) shows the result for the common linear correlation. Note that we have plotted the optical results only for the region of interest of the correlation plane. The SONG correlation detects the target without difficulty, but the linear correlation is not able to discriminate the target from the background.

Another detection case of interest is where the target is in the presence of a highly correlated background, such as buildings. A city image is shown in Fig. 6(b) where the object is to find a specific building.

The SONG correlation for Fig. 6(b) is shown in Fig. 8(a). The building is perfectly isolated from the background. The noise comes from the importance of the zero-order and from the inherent noise in any optical experiment. The typical linear correlation of Fig. 8(b) fails to isolate the target.

The final result is a less common detection problem: imagine that we need to detect an object in the presence of other objects or patterns and the reference object that we used as a filter is itself also surrounded with a background, as in Fig. 6(c); in other words, the reference object is not segmented. Note that this particular case is a priori more difficult to deal with than for the case of the noise-free reference objects. Fig. 9(a) shows the SONG correlation when Fig. 6(c) is introduced into the spatial light modulator. Note that the nonlinear correlation allows detection of the image with high discrimination. Here the linear case also fails, as is shown in Fig. 9(b).

6. Conclusion

We have optically implemented the sliced orthogonal nonlinear generalized (SONG) correlation and we have studied the influence of this correlation on cluttered images and for nonoverlapping background noise patterns. Because the nonlinear SONG correlation is defined by means of a sum of linear correlations between binary images, it can easily be implemented optically with a JTC. We have compared the performances of the SONG auto-correlation with that of the POF and of the IF and we showed among other things the stability of the SONG correlation for different correlation parameters like the PCE and the auto-correlation noise to signal ratio (ANSR). This study shows that the SONG correlation is invariant to almost any changes of the background for cases where the background does not overlap the target. This is verified for the whole correlation plane, not only at the origin. Experimental results were presented for various kind of detection problems and those results were compared with those for optical linear correlation.

Acknowledgements

This work has been supported by the Spanish DGES, Dirección General de Enseñanza Superior, project PB96-1134-C02-02 and by a grant from the Natural Sciences and Engineering Research Council of Canada. P. Garcia-Martinez acknowledges a post-doctoral grant from the Secretaría de Estado de Universidades.

References

[1] B. Javidi, J. Wang, Appl. Opt. 31 (1992) 6826.
[2] B. Javidi, J. Wang, J. Opt. Soc. Am. A. 11 (1994) 2604.
[3] B. Javidi, Ph. Refregier, P. Willet, Opt. Lett. 18 (1993) 1160.
[4] P. Refregier, B. Javidi, G. Zhang, Opt. Lett. 18 (1993) 1453.
[5] P. Garcia-Martinez, H.H. Arsenault, A correlation matrix representation using the sliced orthogonal nonlinear generalized decomposition, Opt. Commun. 172 (1999) 181–192.
[6] P. Garcia-Martinez, D. Mas, J. Garcia, C. Ferreira, Appl. Opt. 37 (1998) 2112.
[7] B.V.K. Vijaya Kumar, L. Hassebrook, Appl. Opt. 29 (1990) 2997.
[8] A. Shemer, D. Mendlovic, G. Shabtay, P. Garcia-Martinez, J. Garcia, Appl. Opt. 38 (1999) 781.